

Acoustic Methods for Obtaining the Pressure Reflection Coefficient from a Buffer Rod Based Measurement Cell

Erlend Bjørndal, *Member, IEEE*, and Kjell-Eivind Frøysa

Abstract—The known acoustic methods for obtaining the pressure reflection coefficient from a buffer rod based measurement cell are presented, along with 2 new generic approaches for measuring the pressure reflection coefficient using 2 buffer rods enclosing the liquid to be characterized in a symmetrical arrangement. An acoustic transducer is connected to each of the buffer rods. The generic approaches are divided into a relative amplitude approach and a mixed amplitude approach. For the relative amplitude approach, families of 4, 5, or 6 echo signals can be used to obtain the pressure reflection coefficient. The mixed amplitude approach uses specific information about the transducers and/or the electronics sensitivities in receive mode to obtain the pressure reflection coefficient using families of 3, 4, 5, or 6 echo signals. Some of the new methods from the relative amplitude approach imply a reduced uncertainty relative to the previously known ABC method. The effect of the liquid attenuation, digitizer bit resolution, and the signal-to-noise ratio on the uncertainty characteristics of the pressure reflection coefficient are discussed, along with a discussion of the suitability of the various methods for different buffer materials.

I. INTRODUCTION

BUFFERS are widely used for material characterization by acoustic means. The motivation may include delay lines for avoiding the transducer's phase aspects in the reflection process [1], the use of buffers for high temperature measurements [2] (then one buffer only is normally exploited), and the use of buffers as reference materials for obtaining the sample's acoustic impedance [3], where the acoustic impedance Z is the product of the sound speed c and the density ρ . Also, buffers made of multiple materials are sometimes used [4], but these tend to reduce significantly the energy of the acoustic wave encountering the sample due to the multiple reflection process [5].

The pressure reflection coefficient (called reflection coefficient for simplicity) has applications in various areas, for example, obtaining the characteristic acoustic impedance and attenuation of both fluids and solids; measurement of liquid density (through the use of the expression for

the plane-wave reflection coefficient); fluid characterization, biomedical diagnostics, process control in the industry; and quality control in the food and beverage industry.

Quite a few methods for the measurement of the reflection coefficient in connection with buffers are known. One method designated here as the air/liquid method [6]–[9] uses a transducer in pulse-echo mode with the transducer element fixed to a buffer. Then, during the calibration phase, 2 measurements are needed. One is performed in air and a second measurement is performed with a sample liquid inserted between the buffer and a reflector. This method has been used to a significant degree, but is known to suffer from the need of frequent calibrations due to thermal drift and aging of the electronics and sensor components [5]. A reference acoustic path would reduce such problems, as part of the transmitted signal would be available for automatic calibration purposes.

In 1968, Papadakis presented 2 methods for measuring the reflection coefficient at the buffer-sample interface and the sample attenuation that both comply with the need of a reference acoustic path [10], [11]. These will here be termed the short-pulse and the long-pulse method for further discussion.

A. Short-Pulse Method

Papadakis [10] developed a pulse-echo method for measuring the reflection coefficient at the buffer-sample interface and the sample attenuation based on a triple-echo buffer rod approach. The reflection coefficient is obtained from the measured amplitude ratios, where the echo signals have traversed the sample liquid 0, 2, and 4 times, respectively. This method may be prone to severe attenuation of the third echo signal because it has traversed the sample 4 times. It suffers also from a possibility of experiencing interfering effects of the echo signals from the ring-down in the case of short buffers or from mode converted echo signals from the buffer-sample interface in the case of long buffers. However, some inherent benefits of this method are that the amplitude ratios are not affected by operating the transducer away from its resonance frequency because none of the echo signals considered arise from reflections at the buffer-transducer interface [10] and that the measurement of the same amplitude ratios are not affected by the acoustic coupling layer between the transducer and the buffer. This method has been quite extensively used for various applications as exemplified by liquid

Manuscript received May 1, 2007; accepted November 1, 2007. This work was supported by the Norwegian Research Council (NFR), Statoil and Gassco through the 4-year SIP "Ultrasonic Technology for Improved Exploitation of Petroleum Resources" (2003–2006).

E. Bjørndal is with 3-Phase Measurements AS, Bergen, Norway (e-mail: erlend.bjorndal@3-phase.no).

K.-E. Frøysa is with Christian Michelsen Research AS, Bergen, Norway.

Digital Object Identifier 10.1109/TUFFC.2008.862

density measurements [12]–[14], high temperature attenuation measurements in metals approaching their melting point [15], for prediction of grain size in copper [16], and for attenuation measurements of sedimentary rocks under high pressure [17], in addition to material characterization of plastics and polymers [18], [19].

B. Long-Pulse Method

This method [11] was primarily intended used in samples that are very thin, perhaps only a few wavelengths thick, where the short-pulse method is not able to distinguish the individual echo signals properly. This method uses a transmit burst signal that is shorter than the round-trip travel time in the buffer but longer than 3 times the round-trip travel time in the sample. The sample and the buffer then act as a multi-path interferometer where the envelope of the returned echo signal shows a stepwise amplitude modulation of one step per round trip in the sample. From the measured amplitudes of the first 3 steps, the reflection coefficient at the buffer-sample interface and the sample attenuation can be obtained. This method does not seem to have been used extensively, although it has been used on thin rods and wires [20]. However, the suitability for this method to be used on samples that are somewhat thicker needs to be discussed. Possible interference effects of the echo signals due to mode converted echo signals from the buffer-sample interface seem unavoidable.

McSkimin [21] proposed the Papadakis short-pulse method [10] as long ago as 1957 using 2 identical buffers for the measurement of sound speed and attenuation in liquids as a function of temperature and pressure and stated the equations involved, but did not explicitly give any expression for, the reflection coefficient. Later, McSkimin and Chambers [22] proposed a slightly modified measurement cell for high-frequency measurements of mechanical properties of plastics, where the far-end buffer was shorter than the buffer between the transducer and the sample. The echo signals arising from multiple reflections in the far-end buffer were used for the calculation of the reflection coefficient, but the multiple reflection characteristics from within the sample seems to have been neglected, because this typically will interfere with the echo signals from within the far-end buffer.

A combination of the air/liquid method and the short-pulse Papadakis method is known [23], but will not be considered further due to the lack of a reference acoustic path for the measurement principle involving measurements on both air and a liquid for obtaining the reflection coefficient.

Also a method using 2 buffers was proposed [24], initially for coupling layer correction, but shown later [25] to be able to give the reflection coefficient at the buffer-sample interface and the sample attenuation, where one of the buffers is exactly twice the thickness of the other. The measurements involved must also here be performed in a sequential manner due to the change of buffer.

Püttmer *et al.* [5] suggested a measurement method for obtaining the reflection coefficient based on using a piezo-

electric transducer element clamped between 2 buffers made of the same material, but of unequal dimensions, using sound radiated from the rear side of the piezoelectric transducer element facing air, serving as a reference acoustic path, and letting the front buffer be exposed against the sample liquid. This method does not need to transmit sound through the sample liquid for the measurement of the reflection coefficient. However, to obtain the sample liquid's sound speed and thereby the liquid's acoustic impedance, a receive transducer was placed on the other side of the liquid. Special constraints must be imposed on the transmit transducer to fulfill the demands for a low Q-factor and the simultaneous connection of buffers on the piezoelectric element's front and rear faces, meaning that commercially available broad-band transducers cannot be used.

The use of a buffer in form of a liquid has also been proposed in connection with measurement of liquid density [26], [27]. Then, a solid layer is used for separating the liquid buffer and the liquid to be measured. By accurately tuning the excitation frequency until a half-wavelength resonance condition exists in the solid layer, aiming at a direct acoustic interface between the 2 liquids, an improved sensitivity can be obtained. However, the claimed results indicate that further work is needed before the full potential of the method can be exploited.

Clearly, the measuring methods for obtaining the reflection coefficient from a buffer rod configuration suffers from nonideal operation to a varying degree, with the short-pulse method developed by Papadakis [10] being a prime candidate for further refinement. To overcome some of the limitations of this method, this work aims to retain the inherent benefits of the method and reduce the mentioned disadvantages by using a symmetrical buffer rod configuration enclosing the sample liquid, with an acoustic transducer fixed to each buffer. This gives increased freedom with respect to the echo signals that can be used for the measurement of the reflection coefficient and the sample attenuation.

Such a configuration has been used before for the measurement of the attenuation of bovine skeletal muscle [28], obtaining the reflection coefficient from the air/liquid method, and in [29] for obtaining the acoustic impedance and the density of gas, specifically, however, in a way that does not use the reflection coefficient directly, but uses an approximation instead. This method will be further discussed below. The measurement configuration discussed here is therefore not novel by itself. However, the combination of the signals and the thorough discussion of the various opportunities that the setup provides are novel.

Section II presents the measuring principle, along with a theoretical description assuming a plane-wave approach. A description of some existing and some new methods for the measurement of the reflection coefficient is given in Section III. Section IV presents an uncertainty analysis of the relative amplitude approach with respect to the reflection coefficient given certain buffer-liquid characteristics. Comments and conclusions are given in Section V.

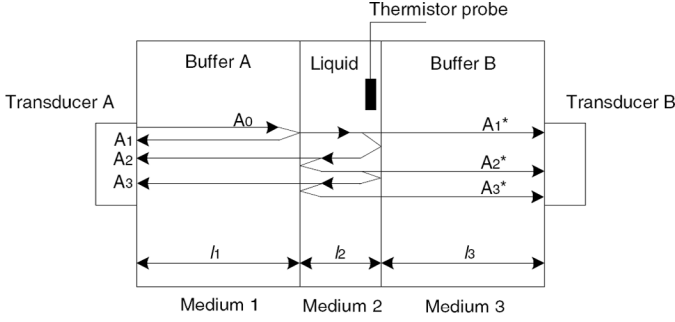


Fig. 1. Schematic view of the proposed measuring principle containing 2 transducers in addition to 2 buffers enclosing the sample liquid. Only the operational mode of using Transducer A in pulse-echo mode is indicated.

II. MEASUREMENT PRINCIPLE

A. Description and Theory of the Proposed Measuring Principle

The description of the measuring principle can be given with respect to Fig. 1, which is seen to consist of one transducer operating in pulse-echo mode (transducer A), together with a receive transducer operating in a through-transmission mode in the other end of the measuring cell (transducer B). The operation can also be reversed, using transducer B in pulse-echo mode, with transducer A as a receiver. Here, a maximum number of 3 echo signals on each transducer will be assumed throughout for the analysis in accordance with the short-pulse Papadakis method [10].

The dimensions of the buffers are assumed to be large enough for multimode propagation to be ignored. Therefore, a plane-wave approach with diffraction correction is taken. These aspects, along with an experimental realization using this measuring principle, are further described in [30].

A fluid-fluid model of the transmission and reflection characteristics will be assumed, implying the satisfaction of 2 boundary conditions: 1) the acoustic pressures on both sides of a boundary are equal, and 2) the particle velocities normal to a boundary are equal [31]. By using a plane-wave approach, the echo signal's amplitudes can be expressed by the reflection and transmission coefficients (R_{ij} and T_{ij} , respectively), for an incident wave in medium i toward medium j with normal incidence. The theoretical formulation assuming attenuation coefficients (α_i) and propagation distances l_i of the buffers and the liquid can be given as

$$A_1 = A_0 R_{12} R_A R_T e^{-2\alpha_1 l_1} \quad (1)$$

$$A_2 = A_0 T_{12} R_{23} T_{21} R_A R_T e^{-2\alpha_1 l_1} e^{-2\alpha_2 l_2} \quad (2)$$

$$A_3 = A_0 T_{12} R_{23}^2 R_{21} T_{21} R_A R_T e^{-2\alpha_1 l_1} e^{-4\alpha_2 l_2}, \quad (3)$$

for the pulse-echo signals on transducer A, along with the corresponding receiver signals

$$A_1^* = A_0 T_{12} T_{23} R_B R_R e^{-\alpha_1 l_1} e^{-\alpha_2 l_2} e^{-\alpha_3 l_3} \quad (4)$$

$$A_2^* = A_0 T_{12} R_{23} R_{21} T_{23} R_B R_R e^{-\alpha_1 l_1} e^{-3\alpha_2 l_2} e^{-\alpha_3 l_3} \quad (5)$$

$$A_3^* = A_0 T_{12} R_{23}^2 R_{21}^2 T_{23} R_B R_R e^{-\alpha_1 l_1} e^{-5\alpha_2 l_2} e^{-\alpha_3 l_3}, \quad (6)$$

on transducer B. When transducer B is used for transmission, the pulse-echo signals are

$$B_1 = B_0 R_{32} R_B R_T e^{-2\alpha_3 l_3} \quad (7)$$

$$B_2 = B_0 T_{32} R_{21} T_{23} R_B R_T e^{-2\alpha_3 l_3} e^{-2\alpha_2 l_2} \quad (8)$$

$$B_3 = B_0 T_{32} R_{21}^2 R_{23} T_{23} R_B R_T e^{-2\alpha_3 l_3} e^{-4\alpha_2 l_2}, \quad (9)$$

whereas the receiver signals appear on transducer A according to

$$B_1^* = B_0 T_{32} T_{21} R_A R_R e^{-\alpha_3 l_3} e^{-\alpha_2 l_2} e^{-\alpha_1 l_1} \quad (10)$$

$$B_2^* = B_0 T_{32} R_{21} R_{23} T_{21} R_A R_R e^{-\alpha_3 l_3} e^{-3\alpha_2 l_2} e^{-\alpha_1 l_1} \quad (11)$$

$$B_3^* = B_0 T_{32} R_{21}^2 R_{23}^2 T_{21} R_A R_R e^{-\alpha_3 l_3} e^{-5\alpha_2 l_2} e^{-\alpha_1 l_1}, \quad (12)$$

where A_0 and B_0 are the incident plane wave pressure amplitudes in front of the sender transducer from each direction consisting of the combined effect of the transducer transmit sensitivity and the acoustic coupling between the transducer and the buffer. A_1 , A_2 , and A_3 are the pressure waves received at transducer A, and A_1^* , A_2^* , and A_3^* are the pressure waves received at transducer B, assuming transducer A is used in pulse-echo mode. The corresponding situation exists for the B_1 , B_2 , B_3 , and for the B_1^* , B_2^* , and B_3^* pressure waves, assuming transducer B is used in pulse-echo mode. Here, R_A and R_B describe the combined effect of the transducer sensitivity and the acoustic coupling between the transducer and the buffer, both in receive mode, for transducer A and transducer B, respectively. The definitions of the R_A and R_B sensitivity factors can be given as the ratio of the plane wave voltage amplitude received by transducer A or B to the plane wave incoming pressure amplitude at transducer A or B. The factors R_T and R_R describe the electronic channel gain as seen by the transducers in receive mode for the transmitter and receiver channel, respectively. The definitions of the R_T and R_R sensitivity factors can be given as the ratio of the plane wave voltage amplitude after preamplifier, for the relevant acquisition channel, to the plane wave voltage amplitude from transducer A or B.

As will be shown below, none of the sensitivity factors applies for the relative amplitude approach, because they disappear in the normalization process. This is, however, not true for the mixed amplitude approach, which uses a different number of echo signals on each transducer.

By assuming identical buffers (indexes $3 \rightarrow 1$) and using the relationships

$$T_{ij} = 1 + R_{ij} \quad (13)$$

$$R_{ji} = -R_{ij}, \quad (14)$$

it is found that (1)–(12) can be expressed as

$$A_1 = A_0 R_{12} R_A R_T e^{-2\alpha_1 l_1} \quad (15)$$

$$A_2 = A_0 R_{12} (R_{12}^2 - 1) R_A R_T e^{-2\alpha_1 l_1} e^{-2\alpha_2 l_2} \quad (16)$$

$$A_3 = A_0 R_{12}^3 (R_{12}^2 - 1) R_A R_T e^{-2\alpha_1 l_1} e^{-4\alpha_2 l_2}, \quad (17)$$

for the pulse-echo signals on transducer A, along with the corresponding receiver signals on transducer B according to

$$A_1^* = A_0 (1 - R_{12}^2) R_B R_R e^{-2\alpha_1 l_1} e^{-\alpha_2 l_2} \quad (18)$$

$$A_2^* = A_0 R_{12}^2 (1 - R_{12}^2) R_B R_R e^{-2\alpha_1 l_1} e^{-3\alpha_2 l_2} \quad (19)$$

$$A_3^* = A_0 R_{12}^4 (1 - R_{12}^2) R_B R_R e^{-2\alpha_1 l_1} e^{-5\alpha_2 l_2}. \quad (20)$$

When transducer B is used for transmission, the pulse-echo signals are

$$B_1 = B_0 R_{12} R_B R_T e^{-2\alpha_1 l_1} \quad (21)$$

$$B_2 = B_0 R_{12} (R_{12}^2 - 1) R_B R_T e^{-2\alpha_1 l_1} e^{-2\alpha_2 l_2} \quad (22)$$

$$B_3 = B_0 R_{12}^3 (R_{12}^2 - 1) R_B R_T e^{-2\alpha_1 l_1} e^{-4\alpha_2 l_2}, \quad (23)$$

and the receive echo signals at transducer A are given as

$$B_1^* = B_0 (1 - R_{12}^2) R_A R_R e^{-2\alpha_1 l_1} e^{-\alpha_2 l_2} \quad (24)$$

$$B_2^* = B_0 R_{12}^2 (1 - R_{12}^2) R_A R_R e^{-2\alpha_1 l_1} e^{-3\alpha_2 l_2}, \quad (25)$$

$$B_3^* = B_0 R_{12}^4 (1 - R_{12}^2) R_A R_R e^{-2\alpha_1 l_1} e^{-5\alpha_2 l_2}. \quad (26)$$

By using (15)–(26), some existing and the new methods will be described in Section III.

B. Nonideal Behavior

The idealized theoretical description given in Section II-A neglects the effects of random and systematic noise and the effect of beam spreading (diffraction). A particular component of the systematic noise is the interference effect from the conversion of shear wave to compressional wave at the buffer-sample interface [32]. Using echo signals that do not interfere with such systematic noise components will be beneficial as the measurement of the echo signal's amplitudes leading to the reflection coefficient otherwise will be in error [30]. Also scattering both from within the buffers and the liquid is ignored. Therefore, a rather pure sample liquid will be assumed to give accurate results.

III. METHODS FOR MEASURING THE REFLECTION COEFFICIENT

A. Introduction

First, the methods known as the air/liquid method and the short-pulse Papadakis method [10] will be described in Sections III-B and III-C, respectively, before the new methods will be given in Sections III-D and III-E. In Section III-F, a further analysis of a method used to obtain the acoustic impedance and the density of gas [29] using the same measuring principle is included.

B. The Air/Liquid Method

This method assumes separate measurements of the echo signal when air is used instead of liquid, with the echo signal given the superscript A index, which combined with a measurement with the sample liquid gives the reflection coefficient. This method requires one transducer connected to a buffer, which again connects with the air or the sample liquid [6]–[9].

Assuming first that these 2 measurements can be performed without having to remount the transducer, and assuming identical acoustic coupling conditions on both transmit and receive in the 2 measurements, the relevant equations can be stated as

$$A_1^A = -A_0^A R_A R_T e^{-2\alpha_1 l_1} \quad (27)$$

for the case of air, assuming a total reflection of the incident sound wave at the buffer-air interface, and

$$A_1 = A_0 R_{12} R_A R_T e^{-2\alpha_1 l_1} \quad (28)$$

for the case of liquid, which gives for the reflection coefficient as

$$R_{12} = -\frac{A_1 A_0^A}{A_1^A A_0}. \quad (29)$$

In practice, the R_A and R_T sensitivity factors will vary due to environmental changes, aging, remounting, and other influences. The effect of this is given in (30)–(32). If the transducer needs to be remounted between the measurements, then the relevant equations read

$$A_1^A = -A_0^A R_A^A R_T^A e^{-2\alpha_1 l_1} \quad (30)$$

for the case of air, and

$$A_1 = A_0 R_{12} R_A R_T e^{-2\alpha_1 l_1} \quad (31)$$

for the case of liquid, giving

$$R_{12} = -\frac{A_1 A_0^A R_A^A R_T^A}{A_1^A A_0 R_A R_T}, \quad (32)$$

indicating that both the transmit and the receive sensitivities for the transducer, the acoustic coupling, and the electronics are involved. From a practical point of view,

the operation of this air/liquid method needs a stable environment. Note also that this method depends solely on the characteristics at the buffer-sample interface, and therefore does not depend on any echo signals that have traversed the liquid path. This method is not included in the further discussion, but primarily included for the sake of completeness and to show the importance of the surrounding equipment on the measurement of the reflection coefficient.

C. The Short-Pulse Papadakis Method

This method was devised in the late 1960s by Papadakis [10] for the purpose of measuring the reflection coefficient at the buffer-sample interface and the acoustic impedance and the attenuation of solids. The characteristics of the buffer are assumed to be known. By using only one transducer and arranging the 3 first echo signals in a certain way, given as

$$\frac{A_1 A_3}{A_2^2} = \frac{R_{12}^2}{R_{12}^2 - 1}, \quad (33)$$

the reflection coefficient can be expressed by

$$R_{12} = \pm \left(1 - \frac{A_2^2}{A_1 A_3} \right)^{-0.5}. \quad (34)$$

This expression can also be found from (15)–(17).

If transmission from both sides is used and combined, as given by

$$\frac{A_1 A_3}{A_2^2} \frac{B_1 B_3}{B_2^2} = \frac{R_{12}^4}{(R_{12}^2 - 1)^2}, \quad (35)$$

cf. (15)–(17) and (21)–(23), the reflection coefficient can be given as

$$R_{12} = \pm \left(1 + \sqrt{\frac{A_2^2 B_2^2}{A_1 A_3 B_1 B_3}} \right)^{-0.5}. \quad (36)$$

Eq. (36) represents a generalization of the short-pulse Papadakis method, using both transducers.

For the short-pulse Papadakis method, we see that none of the acoustic coupling or sensitivity aspects of the transducer or electronics apply, because these factors are cancelled by the fraction $(A_2^2/(A_1 A_3))$. For the further discussion, this method will be designated the ABC method and will serve to a large degree as the reference method for the measurement of the reflection coefficient.

D. Reflection Coefficient Based on a Relative Amplitude Approach

To exploit the echo signals shown in Fig. 1 for obtaining the reflection coefficient, a generic approach will be given using amplitude ratios between 2 or more echo signals on each transducer in a manner that bears resemblance to the

short-pulse Papadakis method [10]. A general relationship can be given according to

$$Y = A_1^a A_2^b A_3^c (A_1^*)^d (A_2^*)^e (A_3^*)^f, \quad (37)$$

where Y is introduced due to convenience, the A -factors are given in (15)–(20), and $a, b, c, d, e,$ and f are independent parameters. To eliminate the transducer sensitivity factors R_A and R_B along with the electronic channel gain factors R_T and R_R , the common A_0 and the $\exp(\alpha_1 l_1)$ factors, 2 relationships are given

$$a + b + c = 0 \quad (38)$$

$$d + e + f = 0. \quad (39)$$

By also eliminating the liquid attenuation term, we obtain the relationship

$$2b + 4c + d + 3e + 5f = 0, \quad (40)$$

from which

$$Y = A_1^a A_2^b A_3^{-a-b} (A_1^*)^d (A_2^*)^{-2a-b-2d} (A_3^*)^{2a+b+d} \quad (41)$$

is obtained. By inserting for the amplitudes (15)–(20), the relationship

$$\begin{aligned} Y &= A_1^a A_2^b A_3^{-a-b} (A_1^*)^d (A_2^*)^{-2a-b-2d} (A_3^*)^{2a+b+d} \\ &= \left(\frac{R_{12}^2}{R_{12}^2 - 1} \right)^a \end{aligned} \quad (42)$$

is found, which without any loss of generality can be written with $a = 1$, as

$$\begin{aligned} Y &= \frac{A_1}{A_2} \left(\frac{A_2}{A_3} \right)^{1+b} \left(\frac{A_1^*}{A_2^*} \right)^d \left(\frac{A_3^*}{A_2^*} \right)^{2+b+d} \\ &= \left(\frac{R_{12}^2}{R_{12}^2 - 1} \right). \end{aligned} \quad (43)$$

It is seen that the echo signal A_1 is a necessary signal in all the possible combinations for the measurement of the reflection coefficient. The general expression for the reflection coefficient based on this relative amplitude approach can be given as

$$\begin{aligned} R_{12} &= \pm (1 - Y^{-1})^{-0.5} \\ &= \pm \left[1 - \frac{A_2}{A_1} \left(\frac{A_3}{A_2} \right)^{1+b} \left(\frac{A_2^*}{A_1^*} \right)^d \left(\frac{A_3^*}{A_2^*} \right)^{2+b+d} \right]^{-0.5} \end{aligned} \quad (44)$$

This equation is seen to have 2 degrees of freedom (b and d), and will be the basis for the further analysis.

From (44) a variety of possible combinations of the echo signals can be found for the measurement of the reflection coefficient. These methods can be broadly classified according to how many different echo signals are used. The different methods are named $R_echoXXX_YYY$ where R stands for the relative amplitude approach, XXX is the

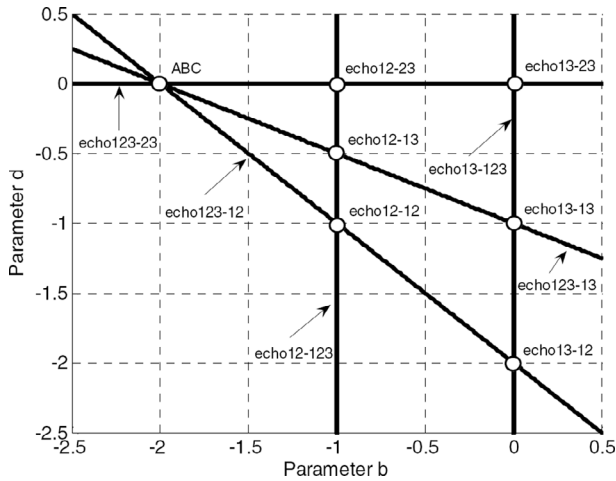


Fig. 2. A 2-D representation of the bd -plane for representing the possible echo signal combination for measuring the reflection coefficient based on 1 transducer and on 2 transducers for the relative amplitude approach.

index of the echo signals used on the transmit transducer, and YYY is the index of the signals used on the receiving transducer. The ABC method is also covered by this formalism, by setting $b = -2$, $d = -0$. This method uses just one transducer and 3 different signals, although the A_2 echo signal appears in the order of 2 to normalize both of the other echo signals. The rest of the methods that will be discussed concerning this approach use 2 transducers and 4, 5, or 6 echo signals.

In Fig. 2, a 2-D diagram of the class of methods for the relative amplitude approach versus the parameters b and d is given. The straight lines represent methods using 5 echo signals, whereas the methods based on 4 echo signals are seen to have a fixed representation in the bd -plane at the location of line crossings. An example of this is the $R_{echo12,12}$ method ($b = -1$, $d = -1$). In general, every point in the bd -plane represents a solution for the reflection coefficient using all of the 6 echo signals. The suitability of these different methods should be given from uncertainty considerations and from possible noise interference characteristics on the echo signals. The different methods can be characterized in the bd -plane according to Table I.

For the $R_{echo12,12}$ method, instead of exploiting the 3 first echo signals on one transducer, one can exploit the combination of the first and the second echo signals on both the transmit and the receive transducer. Also, if interference effects are considered, such as the conversion of shear wave to compressional wave at the buffer-sample interface, one finds an increased flexibility because the involved echo signals occupy a shorter time duration than if 3 echo signals were used.

The $R_{echo13,13}$ method, which uses the first and the third echo signals on both the transmit and the receive transducer, is seen to have some of the same benefits as the $R_{echo12,12}$ method, in that the time frame around the second echo is not used for the calculation of the reflection coefficient. However, the third echo signals will be weaker

TABLE I
CHARACTERIZATION OF MEASURING METHODS FOR THE REFLECTION COEFFICIENT BASED ON THE RELATIVE AMPLITUDE APPROACH.

Method	b	d
ABC	-2	0
$R_{echo12,12}$	-1	-1
$R_{echo12,23}$	-1	0
$R_{echo13,13}$	0	-1
$R_{echo12,13}$	-1	-0.5
$R_{echo13,12}$	0	-2
$R_{echo13,23}$	0	0
$R_{echo12,123}$	-1	Arbitrary
$R_{echo13,123}$	0	Arbitrary
$R_{echo123,12}$	Arbitrary	$-2-b$
$R_{echo123,13}$	Arbitrary	$-1-0.5b$
$R_{echo123,23}$	Arbitrary	0
$R_{echo123,123}$	Arbitrary	Arbitrary

than the second echo signals, to a degree depending on the characteristics of the buffers and the sample liquid, and this method will also be more prone to the effect of liquid attenuation.

E. Reflection Coefficient Based on a Mixed Amplitude Approach

Until now, only methods for the measurement of the reflection coefficient that make use of the relative amplitude approach have been discussed. That is, at least 2 echo signals from each transducer are used to avoid the dependence on the transducer and the electronic sensitivities. However, if a dependence on these sensitivities can be accepted, alternative formulations for the reflection coefficient are possible. If, for instance, one would like to express the reflection coefficient as a function of just one echo signal on one transducer and of 2 echo signals on the other, it is obvious that the transducer and the electronic sensitivities will not be cancelled as in the relative amplitude approach described previously. A generic approach based on this thinking will now be presented. The following relationship can be given:

$$Z = A_1^a A_2^b A_3^c (A_1^*)^d (A_2^*)^e (A_3^*)^f. \quad (45)$$

To eliminate the common A_0 and the $\exp(\alpha_1 l_1)$ factors, a relationship is given:

$$a + b + c + d + e + f = 0. \quad (46)$$

By also eliminating the liquid attenuation term, we obtain the relationship

$$2b + 4c + d + 3e + 5f = 0. \quad (47)$$

Then, e and f can be eliminated to obtain

$$Z = A_1^a A_2^b A_3^c (A_1^*)^d (A_2^*)^{-0.5(5a+3b+c+4d)} \cdot (A_3^*)^{0.5(3a+b-c+2d)}. \quad (48)$$

By inserting for the amplitudes, the relationship

$$Z = \frac{A_1^a A_2^b A_3^c (A_1^*)^d (A_3^*)^{0.5(3a+b-c+2d)}}{(A_2^*)^{0.5(5a+3b+c+4d)}} = \left(\frac{R_A R_T}{R_B R_R}\right)^{a+b+c} \left(\frac{R_{12}^2}{R_{12}^2 - 1}\right)^a \quad (49)$$

is found, which, without any loss of generality can be written with $a = 1$, as

$$Z = \left(\frac{A_1}{A_2}\right) \left(\frac{A_2}{A_3}\right)^{1+b} \left(\frac{A_1^*}{A_2^*}\right)^d \left(\frac{A_3^*}{A_2^*}\right)^{\frac{1}{2}(5+3b+c+2d)} \cdot \left(\frac{A_3}{A_3^*}\right)^{1+b+c} = \left(\frac{R_A R_T}{R_B R_R}\right)^{1+b+c} \frac{R_{12}^2}{R_{12}^2 - 1}. \quad (50)$$

Also here it is seen that the echo signal A_1 is a necessary signal in all the possible combinations for the measurement of the reflection coefficient. Letting $c = -1 - b$, the mixed amplitude approach is seen to be equal to the relative amplitude approach (43), and the relative amplitude approach is a special case of the more general mixed amplitude approach. The general expression for the reflection coefficient can be given as

$$R_{12} = \pm (1 - Z^{-1})^{-0.5} = \pm \left[1 - \left(\frac{R_A R_T}{R_B R_R}\right)^{1+b+c} \cdot \frac{(A_2^*)^{0.5(5+3b+c+4d)}}{A_1 A_2^b A_3^c (A_1^*)^d (A_3^*)^{0.5(3+b-c+2d)}} \right]^{-0.5} \quad (51)$$

This equation is seen to have 3 degrees of freedom. From (51) a variety of possible combinations of the echo signals can be found for the measurement of the reflection coefficient. These methods can be broadly classified according to how many different echo signals are used. The different methods using 3 and 4 echo signals can be characterized in the bcd -space according to Table II. Note that in addition to these methods, there also exist methods based on 5 and 6 echo signals.

A 2-D diagram versus b and d for $c = 0$ is given in Fig. 3. This represents all possible methods where A_3 is not used. That means all possible M_echo12_{123} methods and the subsets of these methods where 3 and 4 echoes are used. The corresponding diagram in the cd -plane ($b = 0$) is given in Fig. 4. This represents all possible methods where A_2 is not used. That means all possible M_echo13_{123} methods and the subsets of these methods where 3 and 4 echoes are used.

TABLE II

CHARACTERIZATION OF MEASURING METHODS FOR THE REFLECTION COEFFICIENT BASED ON THE MIXED AMPLITUDE APPROACH.

Method	b	c	d
M_echo12_{123}	1	0	-2
M_echo12_{12}	-3	0	0
M_echo12_{13}	-5/3	0	0
M_echo13_{123}	0	1/3	-4/3
M_echo13_{12}	0	3	0
M_echo13_{13}	0	-5	0
M_echo1_{123}	0	0	-3/2
M_echo1_{12}	0	0	-5/4
M_echo1_{13}	0	0	0
M_echo12_{12}	Arbitrary	0	$-(3+b)/2$
M_echo12_{13}	Arbitrary	0	$-(5+3b)/4$
M_echo12_{23}	Arbitrary	0	0
M_echo13_{12}	0	Arbitrary	$(-3+c)/2$
M_echo13_{13}	0	Arbitrary	$-(5+c)/4$
M_echo13_{23}	0	Arbitrary	0
$M_echo123_{12}$	Arbitrary	$(1-b)/3$	$-(4+2b)/3$
$M_echo123_{13}$	Arbitrary	$3+b$	0
$M_echo123_{23}$	Arbitrary	$-5-3b$	0
M_echo1_{123}	0	0	Arbitrary

It should be noted that the difference between Fig. 2 and Fig. 3 is that in the relative amplitude approach (Fig. 2), $c = -1 - b$, while in Fig. 3, $c = 0$.

From Figs. 3 and 4 it is seen that the methods using only the first echo signal on the transmit transducer appears in both the bd - and in the cd -planes along the line $b = 0$ and along $c = 0$, respectively.

From (51) it is seen that both the transducer (R_A, R_B) and the electronic sensitivities (R_R, R_T) apply in the receive mode. If, however, the same formalism leading to (51) were applied assuming transmission from both transducers in a sequential manner, and combining the results, then only the electronic sensitivities (R_R and R_T) would appear. As an example of this, consider the M_echo12_{12} method, which by inserting $b = 1, c = 0, d = -2$ in (51), reads

$$R_{12} = \pm \left(1 - \left(\frac{R_A R_T}{R_B R_R}\right)^2 \frac{(A_1^*)^2}{A_1 A_2} \right)^{-0.5} \quad (52)$$

using transmission from one side only. If, however, transmission from both sides of the measuring cell is used, the reflection coefficient reads

$$R_{12} = \pm \left(1 + \left(\frac{R_T}{R_R}\right)^2 \sqrt{\frac{(A_1^*)^2 (B_1^*)^2}{A_1 A_2 B_1 B_2}} \right)^{-0.5} \quad (53)$$

Generally, these 3-echo signal methods seem to represent the minimum amount of echo signals necessary for obtaining the reflection coefficient and seem to be attractive

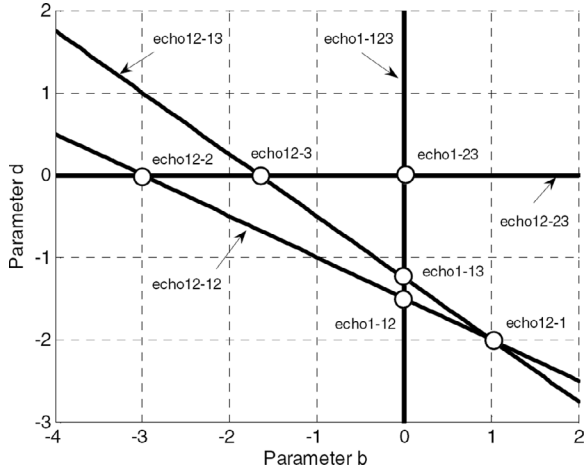


Fig. 3. A 2-D representation of the bd -plane ($c = 0$) for representing the possible echo signal combinations for measuring the reflection coefficient showing the 3 and the 4 echo signal methods for the mixed amplitude approach.

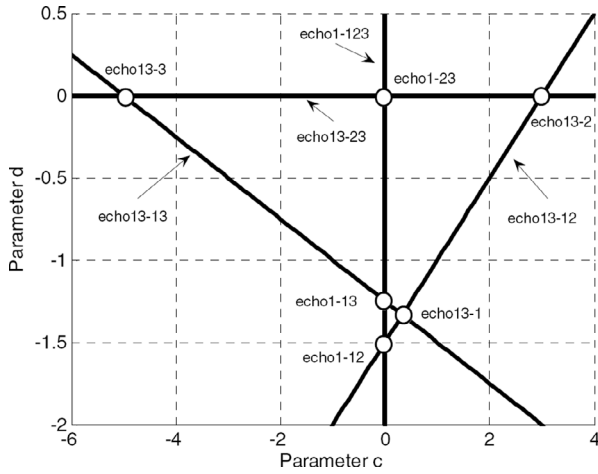


Fig. 4. A 2-D representation of the cd -plane ($b = 0$) for representing the possible echo signal combinations for measuring the reflection coefficient showing the 3 and the 4 echo signal methods for the mixed amplitude approach.

in circumstances such as for very high attenuation liquids, which impedes the transmission of echo signals traversing the one-way liquid path more than twice. In that case, the amplitudes of the A_2 and the A_3 echo signals may approach the noise level due to the combined effect of the reflection process and the attenuation loss. The behavior on the receive transducer is less prone to large amplitude variations between the echo signals because all the echo signals have experienced attenuation loss. Then, methods from the $M_{echo1}YY$ family may be appropriate.

To be operated, the method would have to use sensitivity factors (e.g., $R_A R_T / R_B R_R$ or R_T / R_R) obtained from previous measurements on lower loss liquids or by using direct measurements on the electronics. Another possible inherent benefit of these methods compared with the ABC method is due to the increased flexibility with respect to dimensions of a measurement cell to avoid interference, because the third echo signal does not need to be exploited.

The ratio of the electronics receive sensitivities might be measured directly, depending on the design of the electronics, or found from the echo signals amplitudes using the relationship

$$\left(\frac{R_T}{R_R}\right)^2 = \frac{A_2^2 B_1}{A_1 A_2^* B_1^*} \tag{54}$$

The ratio of the acoustic coupling combined with the transducer sensitivities in receive mode can be obtained as

$$\left(\frac{R_A}{R_B}\right)^2 = \frac{A_1 B_1^*}{A_1^* B_1} \tag{55}$$

A combined expression for the ratio of the acoustic and electronics sensitivities can be obtained using (54) and (55) which gives

$$\left(\frac{R_A R_T}{R_B R_R}\right)^2 = \frac{A_2^2}{A_1^* A_2^*} \tag{56}$$

F. Further Analysis of the Sanderson and Guilbert Patent Application Method for Gas

Sanderson and Guilbert [29] devised a measuring cell based on the same principle as in Fig. 1 for the measurement of the acoustic impedance and the density of a flowing fluid, specifically gas. In their method, the reflection coefficient was not used directly. Instead, the acoustic impedance was found using an approximation of the form $(Z_1 - Z_2) \approx Z_1$, indicating the negligible acoustic impedance of the gas compared with the acoustic impedance of the used plastic buffers, particularly for low gas pressures. Their method uses amplitude ratios that can be shown to lead to the reflection coefficient through the relationship

$$\frac{(A_1^*)^2 B_1^*}{A_1 A_2^* B_1} = \frac{(1 - R_{12}^2)^2}{R_{12}^4} \left(\frac{R_R}{R_T}\right)^2 \tag{57}$$

from which the reflection coefficient can be stated as

$$R_{12} = \pm \left(1 + \frac{R_T}{R_R} \sqrt{\frac{(A_1^*)^2 B_1^*}{A_1 A_2^* B_1}}\right)^{-0.5} \tag{58}$$

and is seen to depend on the electronics receive sensitivities. It is observed that this method uses the first echo signal on the transmit transducer and the first and second echo signals on the receive transducer, in addition to the first echo signal on both the transmit and receive transducer when transmitting from the other side of the measurement cell.

In the case of using transmission from both sides of the measuring cell in a symmetrical manner, as by expanding (57), one obtains

$$\frac{(A_1^*)^2 B_1^* (B_1^*)^2 A_1^*}{A_1 A_2^* B_1 B_1 B_2^* A_1} = \frac{(1 - R_{12}^2)^4}{R_{12}^8} \left(\frac{R_R}{R_T}\right)^4 \tag{59}$$

from which the reflection coefficient can be given as

$$R_{12} = \pm \left(1 + \frac{R_T}{R_R} \sqrt{\frac{A_1^* B_1^*}{A_1 B_1} \sqrt{\frac{A_1^* B_1^*}{A_2^* B_2^*}}} \right)^{-0.5} \quad (60)$$

This method belongs to the mixed amplitude approach, but deviates due to the necessity of transmitting from both transducers. This method can be shown to reduce to the *echo12.12* method of the relative amplitude approach if inserted for the electronics receive sensitivities, i.e., (54) into (57). The main disadvantage of this method is believed to be the necessity of obtaining the ratio of the electronics receiver sensitivities.

IV. UNCERTAINTY ANALYSIS

A. Introduction

To be able to compare the given methods for the measurement of the reflection coefficient rigorously, the uncertainty of each of the methods must be given. Here, only the relative amplitude approach will be detailed. This is done by using the partial derivative approach for the expanded uncertainty U according to

$$U(R) = k \left[\sum_{i=1}^N \left(\frac{\partial R}{\partial x_i} u(x_i) \right)^2 \right]^{\frac{1}{2}}, \quad (61)$$

where u indicates the standard uncertainty, and x indicates the mutual uncorrelated variables on which the reflection coefficient depends. A coverage factor $k = 2$ for a 95% confidence interval is used.

Two measurement cells with water as the sample liquid are proposed for the comparison process. In one of them, the buffers are made of aluminum with an acoustic impedance of $17 \cdot 10^6$ kg/m²s, and in the other the buffers are made of Perspex with an acoustic impedance of $3.2 \cdot 10^6$ kg/m²s [33]. The reflection coefficients for these buffer materials against water are -0.8378 and -0.3617 , for the aluminum buffer cell and for the Perspex buffer cell, respectively. These buffer materials are assumed to have reasonably realistic acoustic parameters because very few alternative materials are available in the low acoustic impedance range for buffer materials. The parameters of aluminum are also found to be quite close to that of quartz glass and Zerodur, which have been found suitable for acoustic measurement of liquid density using a buffer rod configuration measurement cell [34].

B. Relative Amplitude Approach

From (43), it can be shown that

$$\begin{aligned} [u(R_{12})]^2 = & \left(\frac{\partial R_{12}}{\partial Y} \right)^2 \left\{ \sum_{i=1}^3 \left[\left(\frac{\partial Y}{\partial A_i} \right)^2 u(A_i)^2 \right] \right. \\ & \left. + \sum_{i=1}^3 \left[\left(\frac{\partial Y}{\partial A_i^*} \right)^2 u(A_i^*)^2 \right] \right\}, \quad (62) \end{aligned}$$

where

$$\frac{\partial R_{12}}{\partial Y} = -\frac{(R_{12}^2 - 1)^2}{2R_{12}}, \quad (63)$$

and

$$\frac{\partial Y}{\partial A_1} = \frac{Y}{A_1} \quad (64)$$

$$\frac{\partial Y}{\partial A_2} = \frac{b \cdot Y}{A_2} \quad (65)$$

$$\frac{\partial Y}{\partial A_3} = \frac{(-1 - b) \cdot Y}{A_3} \quad (66)$$

$$\frac{\partial Y}{\partial A_1^*} = \frac{d \cdot Y}{A_1^*} \quad (67)$$

$$\frac{\partial Y}{\partial A_2^*} = \frac{(-2 - b - 2d) \cdot Y}{A_2^*} \quad (68)$$

$$\frac{\partial Y}{\partial A_3^*} = \frac{(2 + b + d) \cdot Y}{A_3^* d}. \quad (69)$$

By inserting for (63)–(69) into (62), and dividing by $(R_{12})^2$ to obtain the square of the relative uncertainty, one obtains

$$\begin{aligned} \left[\frac{u(R_{12})}{R_{12}} \right]^2 = & \left(\frac{R_{12}^2 - 1}{2} \right)^2 \left\{ \left[\frac{u(A_1)}{A_1} \right]^2 + \left[\frac{b \cdot u(A_2)}{A_2} \right]^2 \right. \\ & + \left[\frac{(-1 - b) \cdot u(A_3)}{A_3} \right]^2 + \left[\frac{d \cdot u(A_1^*)}{A_1^*} \right]^2 \\ & \left. + \left[\frac{(-2 - b - 2d) \cdot u(A_2^*)}{A_2^*} \right]^2 + \left[\frac{(2 + b + d) \cdot u(A_3^*)}{A_3^*} \right]^2 \right\}. \quad (70) \end{aligned}$$

The uncertainty of the amplitudes can then be split into contributions from quantization and random noise and into a miscellaneous term describing coherent noise contributions according to

$$u(A_1)^2 = u(A_1^q)^2 + u(A_1^{\text{noise}})^2 + u(A_1^{\text{misc}})^2, \quad (71)$$

for the A_1 signal, where the superscript q indicates quantization. The same can be applied for the other signals also. By assuming equal quantization error and equal noise characteristics for the signals of a given transducer, we have

$$u(A_1^q) = u(A_2^q) = u(A_3^q), \quad (72)$$

$$u(A_1^{\text{noise}}) = u(A_2^{\text{noise}}) = u(A_3^{\text{noise}}). \quad (73)$$

This is typically the situation if coherent acquisition of the echo signals from a transducer is used, meaning that all 3 echo signals are acquired simultaneously. The same assumptions are equally applied for the other signals also. By neglecting the miscellaneous contributions, we find that

$$\begin{aligned} \left[\frac{u(R_{12})}{R_{12}} \right]^2 = & \left(\frac{R_{12}^2 - 1}{2} \right)^2 \left\{ \left[\frac{u(A_1^q)^2 + u(A_1^{\text{noise}})^2}{A_1^2} \right] \right. \\ & \left. \cdot B + \left[\frac{u(A_1^{*q})^2 + u(A_1^{*\text{noise}})^2}{(A_1^*)^2} \right] \cdot C \right\}, \quad (74) \end{aligned}$$

where

$$B = 1 + \left(b \frac{A_1}{A_2}\right)^2 + \left[(1+b) \frac{A_1}{A_3}\right]^2, \quad (75)$$

and

$$C = d^2 + \left[(2+b+2d) \frac{A_1^*}{A_2^*}\right]^2 + \left[(2+b+d) \frac{A_1^*}{A_3^*}\right]^2. \quad (76)$$

By inserting for the amplitudes given by (15)–(20), we obtain

$$B = 1 + \frac{b^2 e^{4\alpha_2 l_2}}{(R_{12}^2 - 1)^2} + \frac{(1+b^2) e^{8\alpha_2 l_2}}{R_{12}^4 (R_{12}^2 - 1)^2} \quad (77)$$

and

$$C = d^2 + \frac{(2+b+2d)^2 e^{4\alpha_2 l_2}}{R_{12}^4} + \frac{(2+b+d)^2 e^{8\alpha_2 l_2}}{R_{12}^8}. \quad (78)$$

The effect of finite temporal resolution by the digitizer will be ignored in the further analysis. It can also be noted that

$$\frac{u(A_1^{\text{noise}})}{A_1} = \frac{1}{\text{SNR}_T}, \quad (79)$$

and

$$\frac{u(A_1^{*(\text{noise})})}{A_1^*} = \frac{1}{\text{SNR}_R}, \quad (80)$$

where SNR means the signal to noise ratio, and the subscripts T and R indicate the transmit and the receive transducer, respectively. Also, if the assumption of equal relative error due to quantization applies to both channels, we have

$$\frac{u(A_1^q)}{A_1} = \frac{u(A_1^{*q})}{A_1^*}. \quad (81)$$

By defining

$$X = \frac{\text{SNR}_R}{\text{SNR}_T}, \quad (82)$$

we find that

$$\left[\frac{u(R_{12})}{R_{12}}\right]^2 = \left(\frac{R_{12}^2 - 1}{2}\right)^2 \left\{ \left[\frac{u(A_1^q)}{A_1}\right]^2 (B+C) + \frac{1}{\text{SNR}_T^2} \left(B + \frac{C}{X^2}\right) \right\}. \quad (83)$$

From this, the uncertainty characteristics can be obtained for different signal to noise ratios on each channel. Note also that SNR_T must be applied for the ABC method to be compared with the methods using both transducers.

By considering only the effect of quantization, and thereby assuming a negligible contribution from the noise

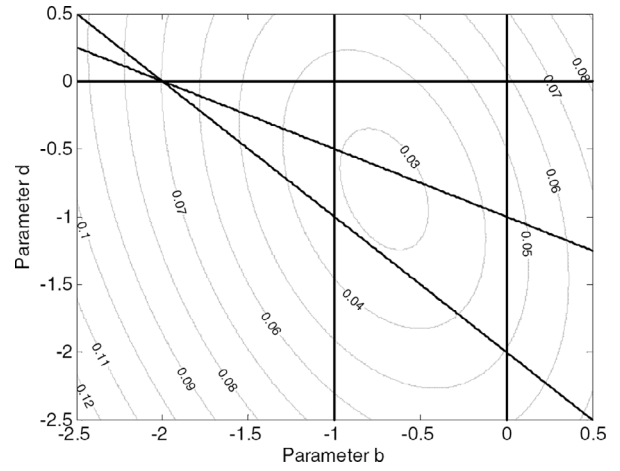


Fig. 5. Expanded relative uncertainty contour plot (in %) for R_{12} for an aluminum buffer cell assuming zero liquid attenuation and a voltage resolution of 12 bits.

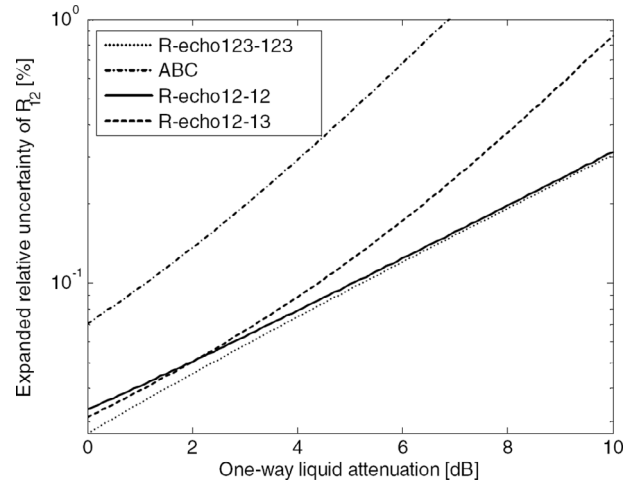


Fig. 6. Expanded relative uncertainty for R_{12} versus one-way liquid attenuation loss for an aluminum buffer cell, using a voltage resolution of 12 bits. Note the logarithmic scale of the y-axis.

term and the miscellaneous term, a simple relationship can be found:

$$\left[\frac{u(R_{12})}{R_{12}}\right]^2 = \left(\frac{R_{12}^2 - 1}{2}\right)^2 \left\{ \left[\frac{u(A_1^q)}{A_1}\right]^2 (B+C) \right\}. \quad (84)$$

In these equations it will be assumed that

$$\frac{u(A_1)}{A_1} = \frac{u(A_1^q)}{A_1} = \frac{1}{2^{N-1}\sqrt{3}}, \quad (85)$$

where $\sqrt{3}$ is due to the rectangular distribution probability function of the quantization process, and N is the number of bits used by the digitizer.

The simulated expanded relative uncertainty of R_{12} for the relative amplitude approach is given in Fig. 5 through Fig. 10, using a voltage resolution of 12 bits and a liquid medium with an acoustic impedance of $1.5 \cdot 10^6$ kg/m²s. In Fig. 5, by ignoring noise, a contour plot of the expanded

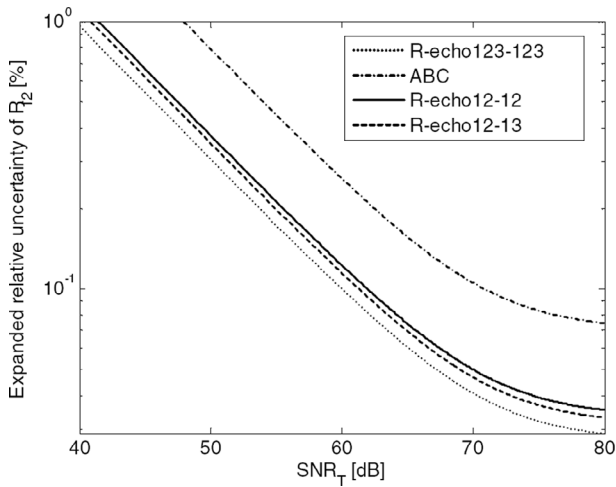


Fig. 7. Expanded relative uncertainty for R_{12} versus SNR for the aluminum buffer cell for zero liquid attenuation, using a voltage resolution of 12 bits. The same SNR is assumed on both transducers. Note the logarithmic scale of the y -axis.

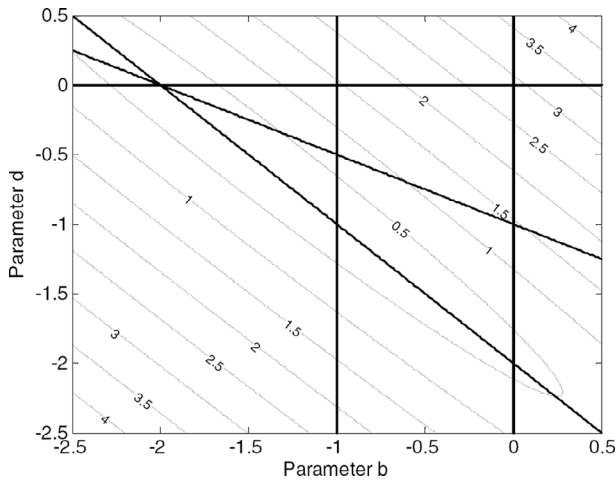


Fig. 8. Expanded relative uncertainty contour plot (in %) for R_{12} for a Perspex buffer cell assuming zero liquid attenuation, using a voltage resolution of 12 bits.

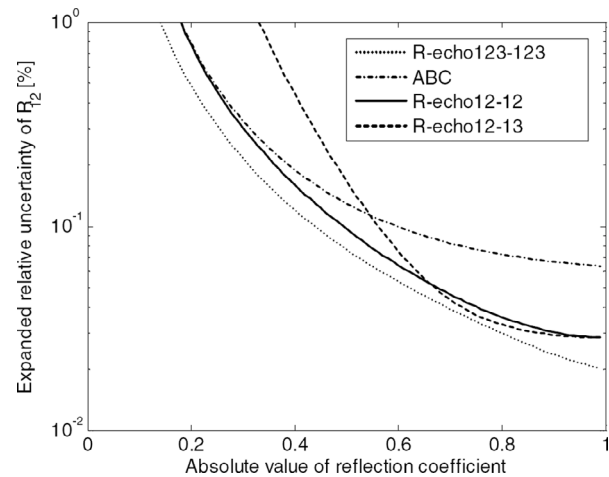


Fig. 9. Expanded relative uncertainty of R_{12} versus $|R_{12}|$ assuming zero liquid attenuation, using a voltage resolution of 12 bits. Note the logarithmic scale of the y -axis.

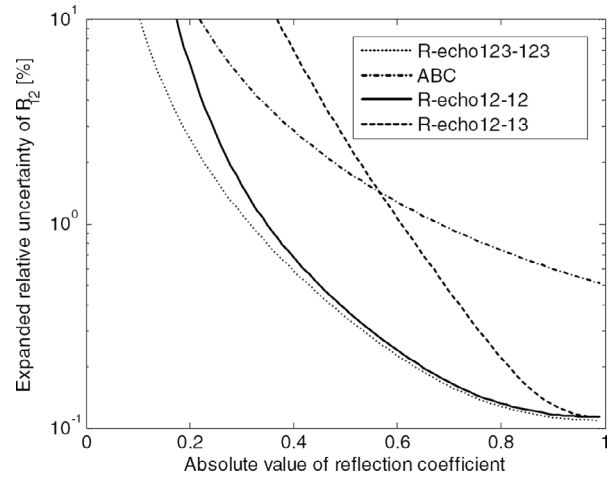


Fig. 10. Expanded relative uncertainty of R_{12} versus $|R_{12}|$ assuming a one-way liquid attenuation of 6 dB, using a voltage resolution of 12 bits. Note the logarithmic scale of the y -axis.

relative uncertainty of R_{12} for an aluminum buffer cell assuming zero liquid attenuation is given. There, the lines for the class of methods for the reflection coefficient according to Fig. 2 versus the parameters b and d are overlaid the contour plot for easier interpretation of the various methods. It is found that the lowest uncertainty is close to the R_{echo12_12} and the R_{echo12_13} method. The point of lowest relative uncertainty uses 6 echo signals (the $R_{echo123_123}$ method) and may in that sense represent the optimum method. For the further quantitative description only, the results from the $R_{echo123_123}$ method along with the ABC method and the R_{echo12_12} and the R_{echo12_13} method are given.

In Fig. 6, the dependence of the expanded relative uncertainty of R_{12} for some methods on the liquid attenuation is given for the aluminum buffer cell. There, it is seen for increasing liquid attenuation that the R_{echo12_12} method has an almost negligible deviation from the relative uncertainty of the optimal and case-dependent $R_{echo123_123}$ method. This behavior of the R_{echo12_12} method deviates largely from the other methods, because they give significantly increased relative uncertainty for higher attenuation. From a practical point of view, this means that the bd -parameters of the optimal and case-dependent $R_{echo123_123}$ method change as the attenuation changes and approaches the bd -parameters of the R_{echo12_12} method for increasing attenuation. Below an attenuation of 2 dB, the R_{echo12_13} method is found to be slightly superior to the R_{echo12_12} method, but significantly worse than the R_{echo12_12} method for a higher attenuation than about 3 dB. At higher values of attenuation, only the R_{echo12_12} method is found to be comparable to the optimal and case-dependent $R_{echo123_123}$ method. A dramatic increase in the expanded relative uncertainty of the ABC method is found compared with the other methods, particularly at increasing attenuation.

Assuming $SNR_T = SNR_R$ —see (79)–(80)—the expanded relative uncertainty characteristics of the reflection

coefficient methods assuming zero attenuation are given in Fig. 7 for the aluminum buffer cell. A flattening of the uncertainty characteristics is observed at a SNR of approximately 70 dB in accordance with the 6 dB per bit rule. For a given SNR, the *R_echo12_12* method is seen to have a lower relative uncertainty than the ABC method.

For the Perspex buffer cell assuming zero attenuation, the expanded relative uncertainty contour plot is given in Fig. 8. A significantly increased relative uncertainty is found compared with the aluminum buffer cell. For the *R_echo12_12* method, this was found to be due to a combination of a high value for dR/dA_2^* , along with a large quantization error of A_2^* , whereas for the ABC method it was due to a high value of dR/dA_3 (relative to the aluminum cell).

Here it is found that the contour describing the lowest uncertainty extends along the line given by the *R_echo123_12* method, making the ABC method better suited for the aluminum buffer measuring cell.

The expanded relative uncertainty of the given methods versus $|R_{12}|$ and assuming zero attenuation is shown in Fig. 9. At the low end of $|R_{12}|$, below about 0.3, the ABC and the *R_echo12_12* method were found to have equal uncertainty. At higher values of $|R_{12}|$, the *R_echo12_12* method split from the ABC method and approached the *R_echo123_123* method. Also, it can be noted that the *R_echo12_13* method is found to have an expanded relative uncertainty marginally lower than the *R_echo12_12* method for $|R_{12}|$ higher than 0.66.

By assigning a one-way attenuation of 6 dB, the uncertainty characteristics versus $|R_{12}|$ change somewhat, as shown in Fig. 10, where only the *R_echo12_12* method is seen to follow the *R_echo123_123* method over a broad range of $|R_{12}|$. The relative uncertainty of the *R_echo12_13* method is also seen to converge to the relative uncertainty of the *R_echo12_12* method only at $|R_{12}|$ approaching 0.9. The point of $|R_{12}|$ at which the ABC method and the *R_echo12_13* method give identical relative uncertainty is seen not to have changed when attenuation increases to 6 dB of one-way loss.

C. Discussion

For a large variety of liquids, a low attenuation value will be experienced. From the figures shown, the relative uncertainty of the different methods is totally different depending on the sample liquid's attenuation and on the value of the reflection coefficient.

For the relative amplitude approach, it is found for the aluminum buffer cell that the *R_echo12_12* method gives a relative uncertainty very close to the optimal and case-dependent *R_echo123_123* method over a very large range of liquid attenuation and therefore avoids the need for precise knowledge of the *bd*-parameters in connection with that *R_echo123_123* method.

Because the mixed amplitude approach needs some additional knowledge about the sensitivity factors to be used, this approach is not believed to be of major importance in

experimental work, and therefore the uncertainty characteristics of this approach will not be presented here.

Finally, it should be noted that no uncertainty contributions from sources of coherent noise, which may contribute to increased uncertainty, and from systematic errors, such as due to diffraction and mode conversion, have been taken into account.

V. COMMENTS AND CONCLUSIONS

It has been shown that the existing methods for measuring the reflection coefficient in a buffer rod configuration measurement cell suffer from the need of performing sequential measurements with different mediums or from using a combination of echo signals that traverses the liquid path multiple times, having an increased possibility of suffering from interference effects and from the effect of liquid attenuation. It has been shown by using 2 buffer rods enclosing the sample liquid in a symmetrical arrangement, and using 2 transducers in a combined pulse-echo and a through-transmission configuration, that these limitations are reduced. Some of the proposed methods seem to have a lower uncertainty associated with them than the reference ABC method, based on analysis of uncertainty contributions from bit resolution and noise only. They seem also to be less exposed to the effect of liquid attenuation. For the relative amplitude approach, the *R_echo12_12* method was found to possess an uncertainty close to the optimal and case-dependent *R_echo123_123* method for widely differing buffer materials. It should also be noted that the relative amplitude approach cancels the effect of the transducer and the electronics sensitivity factors, which is not the case for the mixed amplitude approach.

The main improvements obtained are believed to be the inclusion and the recognition of the effect of the transducers and the electronics sensitivities, along with the proposal of new methods for the measurement of the reflection coefficient. Some of these new methods seem particularly suited for the measurement of high attenuation liquids, and they benefit from being able to obtain a reduced sensitivity of interference effects arising from mode conversion at the buffer-liquid interface, because these methods use a reduced time trace, compared with the ABC method. Experimental verification of some of these new methods in comparison with the ABC method will be given in an accompanying paper regarding acoustic measurement of liquid density [30], with more extensive results given in [35].

REFERENCES

- [1] E. P. Papadakis, K. A. Fowler, and L. C. Lynnworth, "Ultrasonic attenuation by spectrum analysis of pulses in buffer rods: Method and diffraction corrections," *J. Acoust. Soc. Amer.*, vol. 53, no. 5, pp. 1336–1343, 1973.
- [2] E. P. Papadakis, L. C. Lynnworth, K. A. Fowler, and E. H. Carnevale, "Ultrasonic attenuation and velocity in hot specimens by the momentary contact method with pressure coupling,

- and some results on steel to 1200°C," *J. Acoust. Soc. Amer.*, vol. 52, no. 3, pp. 850–857, 1972.
- [3] L. C. Lynnworth and N. E. Pedersen, "Ultrasonic mass flowmeter," in *Proc. IEEE Ultrason. Symp.*, 1972, pp. 87–90.
- [4] J. van Deventer and J. Delsing, "An ultrasonic density probe," in *Proc. IEEE Ultrason. Symp.*, 1997, pp. 871–875.
- [5] A. Püttmer, P. Hauptmann, and B. Henning, "Ultrasonic density sensor for liquids," *IEEE Trans. Ultrason., Ferroelect., Freq. Contr.*, vol. 47, no. 1, pp. 85–92, Jan. 2000.
- [6] L. C. Lynnworth, "Attenuation measurements using the pulse-echo AB method, without multiple echo reverberations in specimen," *Mater. Eval.*, vol. 31, pp. 6–16, Jan. 1973.
- [7] D. J. McClements and P. Fairly, "Ultrasonic pulse echo reflectometer," *Ultrasonics*, vol. 29, no. 1, pp. 58–62, 1991.
- [8] D. J. McClements and P. Fairly, "Frequency scanning ultrasonic pulse echo reflectometer," *Ultrasonics*, vol. 30, no. 6, pp. 403–405, 1992.
- [9] J. Kushibiki, N. Akashi, T. Sannomiya, N. Chubachi, and F. Dunn, "VHF/UHF range bioultrasonic spectroscopy system and method," *IEEE Trans. Ultrason., Ferroelect., Freq. Contr.*, vol. 42, no. 6, pp. 1028–1039, Nov. 1995.
- [10] E. P. Papadakis, "Buffer-rod system for ultrasonic attenuation measurements," *J. Acoust. Soc. Amer.*, vol. 44, no. 5, pp. 1437–1441, 1968.
- [11] E. P. Papadakis, "Ultrasonic attenuation in thin specimens driven through buffer rods," *J. Acoust. Soc. Amer.*, vol. 44, no. 3, pp. 724–734, 1968.
- [12] W. Sachse, "Density determination of a fluid inclusion in an elastic solid from ultrasonic spectroscopy measurements," in *Proc. IEEE Ultrason. Symp.*, 1974, pp. 716–719.
- [13] B. R. Kline, "System and method for ultrasonic determination of density," U.S. Patent 4 991 124, Feb. 5, 1988.
- [14] J. C. Adamowski, F. Buiochi, C. Simon, E. C. N. Silva, and R. A. Sigelmann, "Ultrasonic measurement of density of liquids," *J. Acoust. Soc. Amer.*, vol. 97, no. 1, pp. 354–361, Jan. 1995.
- [15] J. N. C. Chen, E. P. Papadakis, E. H. Carnevale, and C. A. Carey, "High temperature attenuation and modulus measurements," in *Proc. IEEE Ultrason. Symp.*, 1974, pp. 530–533.
- [16] N. Grayeli, F. Stanke, and J. C. Shyne, "Prediction of grain size in copper using acoustic attenuation measurements," in *Proc. IEEE Ultrason. Symp.*, 1982, pp. 954–959.
- [17] K. W. Winkler, "Attenuation and phase velocity spectra in sedimentary rocks under high pressure," in *Proc. IEEE Ultrason. Symp.*, 1982, pp. 1054–1058.
- [18] B.-N. Hung and A. Goldstein, "Acoustic parameters of commercial plastics," *IEEE Trans. Sonics Ultrason.*, vol. SU-30, no. 4, pp. 249–254, July 1983.
- [19] J. E. Carlson, J. van Deventer, A. Scolan, and C. Carlander, "Frequency and temperature dependence of acoustic properties of polymers used in pulse-echo systems," in *Proc. IEEE Ultrason. Symp.*, 2003, pp. 885–888.
- [20] E. P. Papadakis, "Traveling wave reflection methods for measuring ultrasonic attenuation and velocity in thin rods and wires," *J. Appl. Phys.*, vol. 42, no. 7, pp. 2990–2995, June 1971.
- [21] H. J. McSkimin, "Ultrasonic pulse technique for measuring acoustic losses and velocities of propagation in liquids as a function of temperature and hydrostatic pressure," *J. Acoust. Soc. Amer.*, vol. 29, no. 11, pp. 1185–1192, Nov. 1957.
- [22] H. J. McSkimin and R. P. Chambers, "Methods of measuring mechanical properties of plastics with high-frequency ultrasound," *IEEE Trans. Sonics Ultrason.*, pp. 74–84, Nov. 1964.
- [23] E. R. Generazio, "The role of the reflection coefficient in precision measurement of ultrasonic attenuation," *Mater. Eval.*, vol. 43, pp. 995–1004, July 1985.
- [24] P. Palanichamy, C. V. Subramanian, and B. Raj, "Couplant correction for ultrasonic measurements," *Brit. J. NDT*, vol. 31, pp. 78–81, Feb. 1989.
- [25] D. K. Mak, "Comparison of various methods for the measurement of reflection coefficient and ultrasonic attenuation," *Brit. J. NDT*, vol. 33, pp. 441–449, Sep. 1991.
- [26] M. Hirnschrodt, A. von Jena, T. Vontz, B. Fischer, R. Lerch, and H. Meixner, "Time domain evaluation of resonance antireflection (RAR) signals for ultrasonic density measurement," *IEEE Trans. Ultrason., Ferroelect., Freq. Contr.*, vol. 47, no. 6, pp. 1530–1539, Nov. 2000.
- [27] M. Hirnschrodt, A. von Jena, T. Vontz, B. Fischer, and R. Lerch, "Ultrasonic characterization of liquids using resonance antireflection," *Ultrasonics*, vol. 38, pp. 200–205, Mar. 2000.
- [28] D. Shore, M. O. Woods, and C. A. Miles, "Attenuation of ultrasound in post rigor bovine skeletal muscle," *Ultrasonics*, vol. 24, no. 2, pp. 81–87, Mar. 1986.
- [29] M. L. Sanderson and A. R. Guilbert, "Acoustic measurement of fluid properties," U.K. Patent Application GB 2321705 A, 1998.
- [30] E. Bjørndal, K.-E. Frøysa, and S.-A. Engeseth, "A novel approach to acoustic liquid density measurements using a buffer rod based measuring cell," *IEEE Trans. Ultrason., Ferroelect., Freq. Contr.*, vol. 55, no. 8, pp. 1794–1809, Aug. 2008.
- [31] L. E. Kinsler, A. R. Frey, A. B. Coppens, and J. V. Sanders, *Fundamentals of Acoustics*. 3rd ed. New York: John Wiley & Sons, 1982, ch. 6.
- [32] J. P. Weight, "A model for the propagation of short pulses of ultrasound in a solid," *J. Acoust. Soc. Amer.*, vol. 81, no. 4, pp. 815–826, Apr. 1987.
- [33] L. E. Kinsler, A. R. Frey, A. B. Coppens, and J. V. Sanders, *Fundamentals of Acoustics*. 3rd ed. New York: John Wiley & Sons, 1982.
- [34] N. Hoppe, A. Püttmer, and P. Hauptmann, "Optimization of buffer rod geometry for ultrasonic sensors with reference path," *IEEE Trans. Ultrason., Ferroelect., Freq. Contr.*, vol. 50, no. 2, pp. 170–178, Feb. 2003.
- [35] E. Bjørndal, "Acoustic measurement of liquid density with applications for mass measurement of oil," Ph.D. dissertation, Univer. Bergen, Norway, 2007.



Erlend Bjørndal (M'05) was born in Bergen, Norway, on December 31, 1966. He received his diploma in electrical engineering in 1989 and the M.S. degree in physics in 1994 from the University of Bergen, Norway. He received the Ph.D. degree in physics from the University of Bergen, Norway, in 2007.

He worked at Aanderaa Instruments, Bergen, Norway from 1995 to 1997 and at READ Well Services, Bergen, Norway, from 1997 to 2001, as a development engineer.

From 2001 until May 2007, he worked as a scientist at Christian Michelsen Research AS, Bergen, Norway, in the field of acoustic and electromagnetic sensing principles. He is presently employed at 3-Phase Measurements AS, Bergen, working as a project engineer. His research interests include acoustic transducer design, signal processing, and fluid characterization by acoustic means. He holds one patent within the field of acoustic measurement of liquid density.

Dr. Bjørndal is a member of the Norwegian Society of Chartered Technical and Scientific Professionals (Tekna).



Kjell-Eivind Frøysa was born in Aalesund, Norway, on November 16, 1963. He received the M.S. and the Ph.D. degrees in applied mathematics (theoretical acoustics) in 1987 and 1991, respectively, from the University of Bergen, Norway.

He has worked at Christian Michelsen Research AS, Bergen, Norway, since 1993, as a scientist and later also as a program manager in the field of process instrumentation. His research interests include ultrasonic flow metering, ultrasonic quality measurement of oil and gas, ultrasonic process measurements, and propagation of acoustic waves through multiphase media. He holds one patent in the field of acoustic measurement of liquid density, in addition to several refereed papers within linear and nonlinear acoustics.

Dr. Frøysa is a member of the Norwegian Society of Oil and Gas Measurement (NFOGM) and the Norwegian Society of Chartered Technical and Scientific Professionals (Tekna).